

## Classical dynamics and resonance structures in laser-induced dissociation of a Morse oscillator

Yan Gu\* and Jian-Min Yuan

*Department of Physics and Atmospheric Science, Drexel University, Philadelphia, Pennsylvania 19104*

(Received 4 March 1987)

We study laser-induced dissociation of a Morse oscillator by an ir field as a prototype of multi-photon excitation and dissociation of molecular systems. The driving field is modeled both by a sinusoidal interaction term and by a sequence of  $\delta$  impulses. We have found that the latter case yields results which closely resemble those of the former and considerably facilitates the computation and analysis. Primary and a sequence of secondary resonances are found in our classical dynamical study and are analyzed by using Chirikov's nonlinear resonance theory. We have also calculated the dissociation rate as a function of time, dissociation fractions, and half-lives, all for ensembles of initial states uniformly distributed over regions in the phase space. The half-life as a function of the driving field amplitude follows a scaling law with a critical exponent in close agreement with that predicted for the standard map. This fact and the time-dependent dissociation rate reflect the effects on dynamic flows of the partial barriers formed by cantori.

### I. INTRODUCTION

With the development of high-power infrared lasers, there has been considerable interest in investigating the dynamical behavior of a molecular system under intensive laser radiation.<sup>1-8</sup> A prototype in such investigations is a periodically driven Morse oscillator with a Hamiltonian given by<sup>1-4,7</sup>

$$H = p^2/2\mu + D(1 - e^{-\alpha(r-r_e)})^2 - \epsilon(r-r_e)\cos(ft). \quad (1)$$

Because of the high nonlinearity in the potential, the classical dynamics of a driven Morse oscillator can be very complex. On the other hand, due to recent developments of the general theory of dynamical systems, much has been known about the stochastic behavior of the Hamiltonian systems with few degrees of freedom. However, most of the theories developed are either purely mathematical or rigorously valid only for the simplest models such as a driven pendulum. It would be interesting to see how far the conclusions of these theories can be used in the understanding of more realistic models such as a driven Morse oscillator. More specifically, we would like to apply Chirikov's nonlinear resonance theory<sup>9</sup> directly to the analysis of the resonance structures in the Morse oscillator system.

One interesting recent development in nonlinear dynamics is that of the transport theory<sup>10,11</sup> in Hamiltonian systems in which invariant cantor sets called cantori form partial barriers to trajectories.<sup>10-12</sup> This concept of cantori has been incorporated into new theories of unimolecular chemical reactions,<sup>13</sup> and intramolecular relaxation,<sup>14</sup> and been used in the discussions of the photo-dissociation dynamics.<sup>5</sup> One of the objectives of the present paper is to investigate the last process more closely and try to give some quantitative measure of the role played by cantori in the dissociation dynamics of a

Morse oscillator.

To facilitate the computation and analysis we have replaced the sinusoidal driving term in Eq. (1) by an infinite sequence of periodically pulsing terms. This reduces a problem of one-and-one-half degrees of freedom into one of a two-dimensional area-preserving map. An important consideration for this simplification is that a corresponding quantum study can be carried out to give direct comparison between classical and quantum behavior.<sup>4,5</sup>

Organization of this paper is as follows: In Sec. II we present the equations of motion in the way we calculate them. Chirikov's theory is applied to the analysis of the primary and secondary resonance structures seen in the driven Morse oscillator. The area-preserving map is introduced in Sec. III and is used extensively in the calculation of dissociation rates, dissociation fractions, and half-life of ensembles of trajectories. A scaling law is found for the half-life in the vicinity of the critical field strength for global instability. Discussions and summary of results are given in Secs. IV and V. Some details of transformation relations and nonlinear resonance analysis are given in Appendixes A and B.

### II. NONLINEAR RESONANCE ANALYSIS OF A DRIVEN MORSE OSCILLATOR

Hamilton's equations associated with Eq. (1) are given by

$$\begin{aligned} dr/dt &= p/\mu, \\ dp/dt &= -2D\alpha e^{-\alpha(r-r_e)}(1 - e^{-\alpha(r-r_e)}) + \epsilon \cos(ft). \end{aligned} \quad (2)$$

Introducing dimensionless variables defined by

$$\begin{aligned}
x &= 1 - e^{-\alpha(r-r_e)}, \\
y &= p / \sqrt{2D\mu}, \\
\tau &= \alpha \sqrt{2D/\mu} t, \\
A &= \epsilon / (2D\alpha), \\
\Omega &= f \sqrt{(\mu/2D)} / \alpha,
\end{aligned} \tag{3}$$

we can write Eq. (2) into the following form:

$$\begin{aligned}
dx/d\tau &= (1-x)y, \\
dy/d\tau &= -(1-x)x + A \cos(\Omega t).
\end{aligned} \tag{4}$$

Equation (4) is written in a form appropriate for numerical computation. All the calculations reported below will be done for the laser frequency  $\Omega=0.9$  which is red shifted from the Morse frequency, the frequency in the harmonic limit, set to unity in Eq. (4). This value of frequency  $\Omega$  is chosen such that the maximal dissociation rate is generated at a fixed field amplitude  $A$ . By using molecular constants of the HF molecule we can get an idea of the magnitudes of quantities involved here. The Morse frequency equals to  $4138 \text{ cm}^{-1}$  and a field amplitude  $A=1$  corresponds to a laser intensity of  $320 \text{ TW/cm}^2$ .

For the purpose of nonlinear resonance analysis it is more convenient to rewrite Eq. (4) in terms of action-angle variables ( $I$  and  $\theta$ ) of an isolated Morse oscillator. We show in Appendix A that the transformation relations are given by

$$\begin{aligned}
x &= (E + \sqrt{E} \cos\theta) / (1 + \sqrt{E} \cos\theta), \\
y &= -\omega \sqrt{E} \sin\theta / (1 + \sqrt{E} \cos\theta),
\end{aligned} \tag{5}$$

where  $E = I - I^2/4$  is the dimensionless energy of the unperturbed Morse oscillator and

$$\omega = \partial E / \partial I = 1 - I/2$$

is the natural frequency of the oscillator. We note that  $E$  has a value between 0 and 1 for a bound state.

In terms of new variables the Hamiltonian becomes<sup>7</sup>

$$\begin{aligned}
H' = H/D &= E - 2A \ln[(1 + \sqrt{E} \cos\theta)/(1 - E)] \cos(\Omega\tau) \\
&= E - 2A \sum_{n=0}^{\infty} f_n(E) \cos(n\theta) \cos(\Omega\tau),
\end{aligned} \tag{6}$$

where

$$\begin{aligned}
f_0(E) &= (1/\pi) \int_0^\pi \ln[(1 + \sqrt{E} \cos\theta)/(1 - E)] d\theta \\
&= \ln\{[1 + \sqrt{(1-E)}] / [2(1-E)]\} \\
f_n(E) &= (2/\pi) \int_0^\pi \cos(n\theta) \ln[(1 + \sqrt{E} \cos\theta)/(1 - E)] d\theta \\
&= -(2/n) \{-\sqrt{E} / [1 + \sqrt{(1-E)}]\}^n, \quad n = 1, 2, \dots
\end{aligned}$$

We begin the analysis by considering first the primary resonances. Substituting  $\omega\tau$  for  $\theta$  on the right-hand side of Eq. (6), we obtain conditions for occurrences of primary resonances

$$n\omega(I) \pm \Omega = 0. \tag{7}$$

The standard theory<sup>9</sup> gives the following formula of the resonance width:

$$\Delta I = 4\sqrt{2|Af_n(E)|}, \tag{8}$$

where  $E$  denotes the energy determined by Eq. (7).

In Fig. 1(a) we present surface-of-section plots of 14 trajectories of Eq. (4) in the  $E$ - $\theta$  plane where  $\Omega=0.9$  and  $A=0.025$ . We list also the resonance locations and widths predicted by the theory in Table I. We see that the calculated locations and widths of the first two primary resonances with the winding number  $\omega/\Omega=1/1$  and  $1/2$  are approximately given by the theory. Table I also shows that  $1/2$  and  $1/3$  resonances do overlap with each other. This explains why the  $1/3$  resonance has not been found. In fact all the phase points lying in the stochastic layer around the  $1/2$  resonance islands dissociate within a few optical cycles. This implies that no bounding torus exists between the  $1/2$  resonance region and the continuum where  $E > 1$ . Furthermore, a global stochastic instability sets in when  $1/2$  and  $1/1$  resonances overlap. The critical field strength for the global instability predicted by Eq. (8) is  $A_c^{\text{theo}} \approx 0.0605$ . This can only be considered as an order of magnitude estimate, which is usually too large. Numerical simulation yields

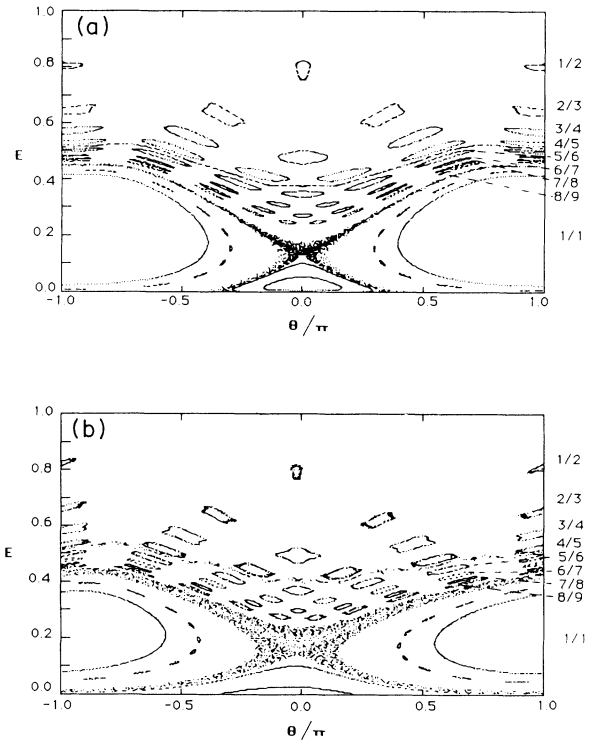


FIG. 1. Surface-of-section plots for a driven Morse oscillator with the driving frequency set at  $\Omega=0.9$ . The winding numbers of some of the trajectories in the resonance regions are labeled on the right-hand side of the plot. (a) Trajectories calculated from differential equation (4) with  $A$  set at 0.025, which is slightly below the critical field strength. (b) Trajectories from map (13) with the driving strength  $a$  fixed at 0.03, which is slightly above the critical value.

TABLE I. Locations and widths of the first three primary resonances of a driven Morse oscillator with  $\Omega=0.9$  and  $A=0.025$ .

Winding number $\omega/\Omega$	1/1	1/2	1/3
Resonance location $E$	0.19	0.7975	0.91
Resonance width $\Delta E$	0.4535	0.1720	0.0850

$A_c^{\text{exp}} \leq 0.0292$ . The discrepancy between the theory and numerical experiment is due to the fact that the phase variable  $\theta$  depends linearly on time only in the zeroth-order approximation. The resonance structures of a driven Morse oscillator are actually much more complicated than those which appear explicitly in the Hamiltonian.<sup>9</sup> Indeed, in Fig. 1(a) a sequence of secondary resonances with the winding number given by  $\omega/\Omega=(n-1)/n$ ,  $n=3,4,5,\dots$  can clearly be seen between the 1/1 and 1/2 resonance regions.

To understand the appearance of this sequence of secondary resonances, we consider below the interaction between the 1/1 and 1/2 resonances and neglect all other resonance and antiresonance terms in the Hamiltonian (6).<sup>15</sup> We write the Hamiltonian in the following form:

$$H' = E - Af_1(E)\cos(\theta - \Omega\tau) - Af_2(E)\cos(2\theta - \Omega\tau). \quad (9)$$

Assuming that  $f_1(E)$  and  $f_2(E)$  are constants we can perform a time-dependent canonical transformation

$$\begin{aligned} I &\rightarrow \hat{p} = I - 2(1 - \Omega), \\ \theta &\rightarrow \hat{\theta} = \Omega\tau - \theta - \pi \end{aligned}$$

to transform Hamiltonian (9) into a form for a driven pendulum

$$K(\hat{p}, \hat{\theta}) = \hat{p}^2/4 - 2\omega_0^2 \cos \hat{\theta} - \beta \cos(2\hat{\theta} - \Omega\tau), \quad (10)$$

where  $\omega_0 = \sqrt{Af_1/2}$ ,  $b = -Af_2$ .

We show in Appendix B that by examining the motion in the vicinity of the pendulum separatrix system (10) displays an infinite sequence of secondary resonances near the separatrix as a result of the breakup of those tori whose frequency is an integer submultiple of the driving frequency, namely,  $\hat{\theta} = \Omega\tau/n$ ,  $n=2,3,4,\dots$ . Transforming back to the original system (9) we obtain

$$\theta = (n-1)\Omega\tau/n + \pi$$

or

$$\omega\Omega = (n-1)/n, \quad n=2,3,4,\dots$$

Thus this analysis correctly predicts the winding numbers of the secondary resonances.

To go one step further we can estimate the critical field strength  $A_c$  at which the global instability sets in based on the overlap criterion.<sup>9</sup> The locations and widths of these resonances are given, as shown in Appendix B, by the following formulas:

$$\begin{aligned} w &= 64\omega_0^2 e^{-2\pi n/\lambda}, \\ \Delta w &= 32\omega_0 \sqrt{(\mu/\lambda)} e^{-\pi n/\lambda}, \end{aligned} \quad (11)$$

where  $w$  measures the distance to the pendulum separatrix in unit of dimensionless energy and

$$\begin{aligned} \lambda &= \Omega/\omega_0, \\ \mu &= (16\pi/3)\lambda^4 \beta e^{-\pi\lambda/2}. \end{aligned}$$

From Eqs. (11) we conclude that the resonance width decreases more slowly with  $n$  than the spacing between resonances. Therefore for any values of the perturbation strength there always exists a stochastic layer in the neighborhood of the unperturbed pendulum separatrix in which the overlap does take place. But the global instability sets in only after the 1/2 and 2/3 resonances overlap with each other. If we use the values of  $f_1$  and  $f_2$  at the location of the 1/1 resonance, we can obtain from Eq. (11) the critical perturbation strength  $A_c^{\text{theo}} \approx 0.16$  for the global instability. Unfortunately this value is farther away from the numerical value than that predicted based on the primary resonances alone. The large discrepancy is obviously caused by the assumption that  $f_1$  and  $f_2$  are constants. To improve the prediction higher-order approximations which take into consideration the energy dependence of  $f_1$  and  $f_2$  should be used.

Numerical calculations show that at  $A=0.025$  resonance regions associated with the winding number  $\omega/\Omega=1/2$ ,  $2/3$ , and  $3/4$  do overlap while resonances with higher winding numbers are still separated from them by Kolmogorov-Arnol'd-Moser (KAM) tori [a trajectory between the 4/5 and 5/6 resonance regions is shown in Fig. 1(a) which is believed to be a bounding KAM torus]. It seems that in the present case the winding number of the most robust KAM torus which is the last torus to break up when  $A$  reaches the critical value  $A_c$  is an irrational number between 0.8 and 1. This situation is different from that in the standard map where the most robust KAM torus has a winding number given by  $(\sqrt{5}-1)/2$ , the golden mean.<sup>16</sup>

### III. DISSOCIATION DYNAMICS AND EVIDENCE FOR THE SCALING BEHAVIOR NEAR DISSOCIATION THRESHOLD

Using the driven Morse oscillator as a model we shall investigate in this section the molecular dissociation process induced by an intense laser field. We consider a trajectory as being dissociated once its dimensionless energy becomes greater than 1. The support of this definition of dissociation comes from numerical calculations. Due to the short-range nature of the Morse potential de-excitation, restabilization of a trajectory which is on its way to dissociate is thus very unlikely. A more sophisticated definition of dissociation can be introduced at a later stage.

As mentioned in Sec. II, when driving strength is increased beyond a critical value, all resonances overlap and a global instability sets in. This critical phenomenon dictates the existence of a dissociation threshold for the low-lying states of a molecular system.

This threshold can be disclosed by physical and numerical experiments.

Since numerical simulations of a dissociation process near threshold by using differential equations are time consuming, we shall replace the sinusoidal driving term in Eq. (4) by the following infinite sequence of periodic impulses:

$$a \sum_{n=-\infty}^{\infty} \{ \delta(\tau - 2n\pi/\Omega) - \delta[\tau - (2n+1)\pi/\Omega] \} \\ = (2a\Omega/\pi) \sum_{n=1}^{\infty} \cos(2n-1)\Omega\tau. \quad (12)$$

With this change the motion of the oscillator on the surface of section can be described by the following two-dimensional mapping:

$$M = S^* K^{-1} S^* K, \quad (13)$$

where  $K$  represents the mapping at the impulse and  $S$  that of the free evolution. They are given explicitly by

$$K(x, y) = (x, y + a), \quad (14) \\ S(E, \theta) = [E, \theta + \pi\sqrt{(1-E)/\Omega}].$$

We note that Eq. (12) shows that by using the periodically pulsing form we have introduced infinitely many higher harmonic frequencies of the driving field into the equation. However, because the natural frequency of the Morse oscillator is always less than 1, with the driving frequency fixed at 0.9 the leading term with the fundamental frequency should dominate. We thus expect that differential equations (4) and mapping (13) yield approximately the same results. In Fig. 1(b) we show 14 orbits of mapping (13) in the  $E$ - $\theta$  plane with  $a$  and  $\Omega$  fixed at 0.03 and 0.9. The similarity between the phase portraits displayed in Figs. 1(a) and 1(b) is clearly seen.

We have calculated the trajectories of map (13) for an ensemble of initial points densely and uniformly distributed over an energy curve in the  $E$ - $\theta$  space for several initial energies. Any trajectory whose energy becomes greater than 1 is removed from the ensemble and the fractions of trajectories left after  $N$  iterations are recorded as  $P(N)$ . Since the trajectories with initial points lying inside a stability domain will never dissociate,  $\lim_{N \rightarrow \infty} P(N)$  is generally a positive number. We define the dissociation fraction of an ensemble as

$$F = 1 - \lim_{N \rightarrow \infty} P(N).$$

In Table II we list the calculated dissociation fractions for several quantum energy levels of an HF molecule

$$E_n = (n + \frac{1}{2})\nu - (n + \frac{1}{2})^2\nu^2/4, \quad (15)$$

where  $\nu = \sqrt{(2/\mu D)\alpha} = 0.083786$ . We used  $10^4$  trajectories for each ensemble and the limiting value is calculated after 5000 iterations which is about 20 times of the average half-life of an ensemble. Two pronounced minima of the dissociation fractions located at quantum numbers  $n=2$  and 13 can be seen in Table II. They are caused clearly by the presence of the 1/1 and 1/2 resonances. A less pronounced one at  $n=9$  close to the 2/3

TABLE II. Dissociation fractions of a Morse oscillator at different energy levels for laser strength  $a=0.06$  and laser frequency  $\Omega=0.9$ .

$n$	$E$	$F = 1 - P(5000)$
0	0.041 45	0.9290
1	0.121 73	0.5791
2	0.198 50	0.5314
3	0.271 75	0.5765
4	0.341 50	0.6693
5	0.407 73	0.7947
6	0.470 46	0.9486
7	0.529 67	0.9983
8	0.585 38	0.9992
9	0.637 57	0.9880
10	0.686 26	0.9998
11	0.731 43	0.9999
12	0.773 10	0.9999
13	0.811 26	0.9763
14	0.845 90	0.9986
15	0.877 04	1.0000

resonance is also recognizable.

The dissociation rate of an ensemble of initial states can be defined by the expression

$$R(N) = -[1/P(N)]dP(N)/dN.$$

For an exponentially decaying ensemble  $R$  is a constant. However, for the system of interest here the dissociation rate not only varies with time, but also depends sensitively on its initial conditions. We plot in Fig. 2 the dissociation rate as a function of time for four ensembles of trajectories with essentially four different initial energies.

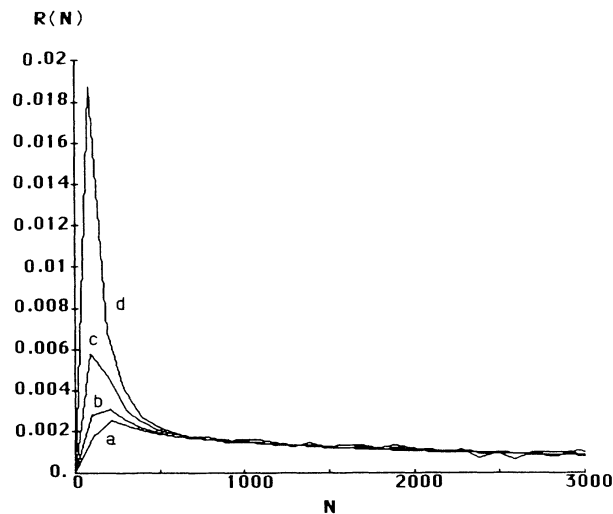


FIG. 2. Dissociation rate as a function of time for ensembles of  $3.6 \times 10^5$  trajectories with initial points uniformly distributed in small squares located at  $\theta=0$  and (a)  $E=0.04145$ , (b)  $E=0.1985$ , (c)  $E=0.2718$ , (d)  $E=0.4077$ . The driving strength and frequency are  $a=0.06$  and  $\Omega=0.9$ .

Each ensemble contains  $3.6 \times 10^5$  initial points distributed in a square box of length 0.0001 in the  $E$ - $\theta$  plane. To suppress the fluctuations in statistics we have presented average values of  $R$  over a hundred iterations. A remarkable fact disclosed in this figure is that all these four curves converge quickly to a common dissociation rate which appears to decrease gradually with time. This fact can be understood by invoking the theory of transport in Hamiltonian systems developed by Mackay *et al.*<sup>10</sup> and Bensimon and Kadanoff.<sup>11</sup> According to this theory, beyond the onset of the global instability invariant cantor sets called cantori, remnants of tori, still exist in the phase space. They form partial barriers to the stochastic phase flows. Due to the obstructions of these partial barriers, ensembles of trajectories initiated at different locations of the phase space approach a common quasiequilibrium state which yields essentially the same dissociation rate. In Fig. 3 we show several ensembles of trajectories at selected times. Figures 3(a) and 3(b) are results of an ensemble initially located at  $E=0.04145$  and  $\theta=0$ . Figures 3(c) and 3(d) belong to another ensemble initially at  $E=0.27175$  and  $\theta=0$ . Although after a short time evolution (40 iterations) the two distributions generated from these two ensembles

are different [Figs. 3(a) and 3(c)], they become quite similar after 400 iterations as shown in Figs. 3(b) and 3(d). Also recognizable are the partial barriers from the sudden change of density in these distributions.

An important conclusion of the transport theory is that the flux through the gaps (or turnstiles) of the tori satisfies a universal scaling law for the parameter  $a$  above and close to its critical value,  $a_c$ , of the global instability. In order to test this scaling law half-lives of an ensemble of initial points within a dense distribution located at  $E=0.1985$  and  $\theta=0$  have been calculated as a function of  $a$ . Numerical results are presented in Fig. 4, in which we plot the half-life,  $N_{1/2}$ , as a function of  $a$ . We have found by the least-square method that our data are best fitted by the following straight line given by

$$\ln N_{1/2} = -\eta \ln(a - a_c) + B,$$

where the fitted constants for 18 data points with  $a \leq 0.038$  are

$$a_c = 0.025,$$

$$\eta = 3.01,$$

$$B = -4.53.$$

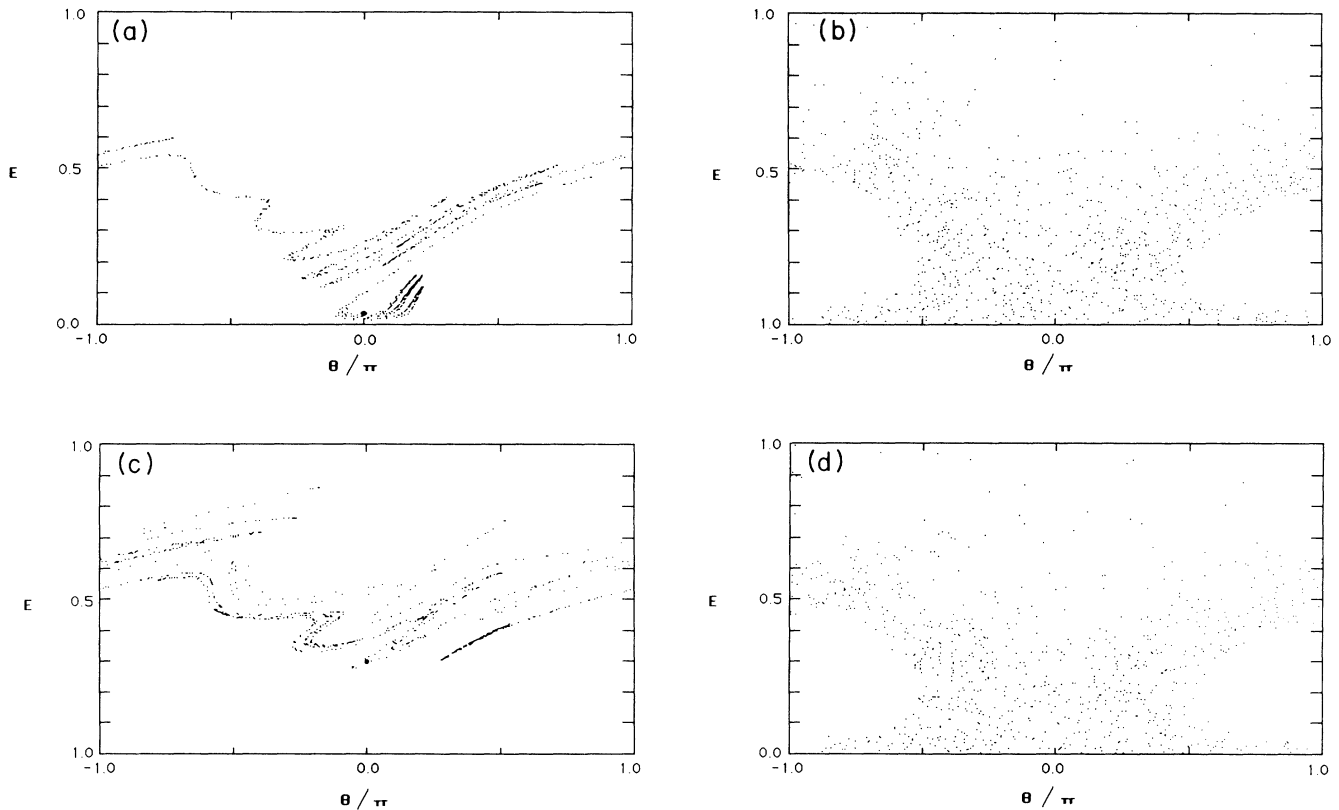


FIG. 3. Diffusion of an ensemble of  $10^3$  trajectories initially confined in a region of dimension 0.0001, indicated in (a) and (c) by a solid circle. For (a) and (b) the initial distribution is located at  $E=0.04145$ ,  $\theta=0$ : (a) the distribution after 40 iterations, (b) the distribution after 400 iterations. For (c) and (d) the initial distribution is located at  $E=0.2718$ ,  $\theta=0$ : (c) the distribution after 40 iterations, (d) the distribution after 400 iterations. The parameters  $a$  and  $\Omega$  are the same as given in Fig. 2.

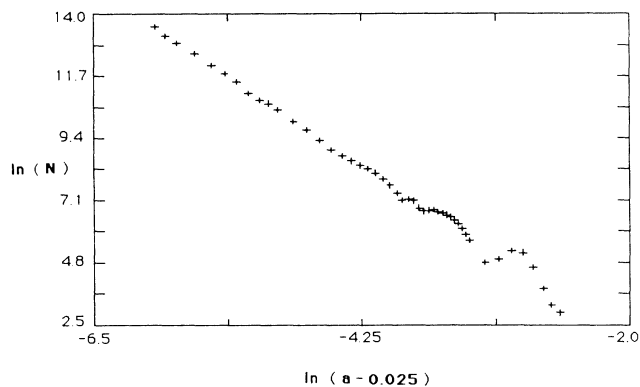


FIG. 4. Dissociation half-life  $N_{1/2}$  of the Morse oscillator as a function of the driving strength  $a$ . The driving frequency is set at  $\Omega=0.9$  and the initial distribution is located at  $E=0.1985$  and  $\theta=0$ .

If we change the range of data points for fitting, the value of  $a_c$  changes only slightly, while  $\eta$  changes from 3.24 (10 data points with  $a \leq 0.031$ ) to 2.85 (all 47 data points used with  $a \leq 0.1$ ). The critical exponent  $\eta$  can be compared with the value  $\eta^{\text{theo}} \cong 3.0117$  predicted by the scaling theory for the standard map.<sup>10</sup> The last bounding torus observed here is not one with the winding number equal exactly to the golden mean, but maybe equal to a number related to it. The good agreement between the theory and our numerical results provides more evidence of the universality of the scaling law.

#### IV. DISCUSSIONS

Since the natural frequency of the Morse oscillator depends on the energy in a square-root relation, Eq. (A3), in principle, there exists an infinite sequence of primary resonances given by  $1/n$ , for any positive integer  $n$  and the positions of these resonances converge to the field-free dissociation limit. In reality these resonances overlap with one another for any finite driving amplitude; therefore we will only see a finite number of them. In the cases of Fig. 1(a) and 1(b) we have found only the  $1/1$  and  $1/2$  resonances. The infinite number of secondary  $(n-1)/n$  resonances generated via the interaction of these two primary resonances, on the other hand, converge to the separatrix of the  $1/1$  resonance. The overlap between them yields the chaotic layers around the separatrix. Therefore it is not an accident that at the stage of overlapping of Fig. 1 few bounding tori or cantori can be found. The torus with a winding number between  $4/5$  and  $5/6$  shown in Fig. 1(a) is a bounding torus, because the  $A$  value used there is below  $A_c$ . All trajectories (or states) initiated below this torus will remain trapped below it, while those initiated above it (except those which fall inside the quasiperiodic domains) dissociate very quickly. Thus the last bounding torus acts as the effective dissociation limit for the oscillator + field system, or the quasidissociation limit. The bounding torus shown in Fig. 1(b), on the other hand, has already started to break up; therefore it is ac-

tually a cantorus. The partial barriers almost recognizable in Figs. 3(b) and 3(d) belong to this kind of cantori, but they have further evolved in the breakup process.

To see the effects of cantori on measurable quantities of a dissociation process, we have calculated the dissociation rate as a function of time and the half-life as a function of the driving amplitude. The common asymptote approached from states with very different energies shown in Fig. 2 is a clear signal of the existence of cantori. The dissociation rate there should be a rather good measure of the flow rate through the cantori. But the value there does not approach a constant, instead it decreases gradually. This slow decay may actually reflect the fact that increasingly finer structures exist in the vicinity of the cantori. The explicit calculation of the scaling law further quantifies the lifetime-driving-amplitude relation as affected by the cantori.

The above two properties and the results of the dissociation fractions of ensembles of trajectories originated on energy curves with the energies given by the eigenstates of a Morse oscillator can all be tested against quantum results and experimental measurements. Of course, it is well known that the laser intensity required to dissociate a diatomic molecule is far too high to be practical, but we hope some of the phenomena that we have discussed here, especially the scaling law found, is universal to all molecular photodissociation processes.

One final note is that the Franck-Condon principle is not applicable to the multiphoton process discussed here. In fact, our results show that for the low-lying states trajectories originated near the inner turning point ( $\theta = \pm\pi$ ) have very little or zero chance to dissociate. On the other hand, trajectories originated near the outer turning point ( $\theta = 0$ ) have the best chance to get to the dissociation region.

#### V. SUMMARY

In this paper we present numerical results of the stochastic behavior of the Hamiltonian system of a Morse oscillator and attempt to understand them based on existing theories. Two aspects are of special interest. One is the resonance structures displayed by the phase-space trajectories. By selecting the appropriate laser frequency and intensity, we have found that between the  $1/1$  and  $1/2$  resonance regions there exists a whole sequence of secondary resonances with the winding number given by  $(n-1)/n$ ,  $n=3,4,5,\dots$ . The existence of such a sequence can be understood by applying the classical resonance analysis<sup>9,15</sup> to a periodically driven pendulum model. However, a straightforward application of this analysis does not yield good predictions of the half-widths of resonances or spacings between them. As a result, the prediction of the onset of the global instability is not better, in fact is even worse, than that predicted by applying the overlap criterion to the primary resonances alone.

Another aspect that we have focused on is the dissociation dynamics of a driven Morse oscillator. As laser intensity increases beyond a critical value, all resonances overlap and global instability sets in. Dissociation of a molecular system can be interpreted as a consequence of

this global instability and can therefore be elucidated by applying the transport theory in the Hamiltonian systems recently developed for the area-preserving maps.<sup>10,11</sup>

To facilitate numerical computation we have replaced the sinusoidal term in system (1) by an infinite sequence of periodical impulses so that the dynamics can be described by an area-preserving map. This makes it possible for us to follow the evolution of a thousand to hundreds of thousands of trajectories at the same time to get statistically meaningful results. The dissociation rate thus obtained not only varies with time, but also depends heavily on the initial conditions. But very interestingly the dissociation rates associated with different initial energies may converge quickly to a common value, which decreases slowly with time. This fact indicates the existence of cantori which form partial barriers to the stochastic flows.

We have also calculated half-lives of ensembles of trajectories for laser intensities slightly above the dissociation threshold for low-energy states. A scaling relation was found with a critical exponent in good agreement with that predicted by the scaling theory.<sup>10</sup>

#### ACKNOWLEDGMENTS

We are grateful to Professor Bai-lin Hao and Mr. James F. Heagy for helpful discussions. This work was supported by the Donors of the Petroleum Research Fund, administered by the American Chemical Society, and by the Army Research Office under Contract No. DAAG29-85-K-0256.

#### APPENDIX A: TRANSFORMATION RELATIONS BETWEEN $(E, \theta)$ AND $(x, y)$

The dimensionless energy  $E$  is defined by dividing the energy  $H_0$  of the field-free oscillator by the dissociation energy  $D$ :

$$E = H_0/D = p^2/(2\mu D) + (1 - e^{-\alpha(r-r_e)})^2 = x^2 + y^2. \quad (\text{A1})$$

The last relation follows from the definitions of  $x$  and  $y$ . The dimensionless action  $I$  is defined by dividing the action by  $D$  and the inverse of the Morse frequency, that is,

$$\begin{aligned} I &= [\alpha\sqrt{(2/D\mu)}/(2\pi)] \oint p \, dr \\ &= (1/\pi) \oint y/(1-x) \, dx \\ &= (1/\pi) \int_{-\pi}^{\pi} E \sin\phi/(1-\sqrt{E} \cos\phi) \, d \cos\phi \\ &= 2[1 - \sqrt{(1-E)}]. \end{aligned} \quad (\text{A2})$$

Thus it follows that

$$\begin{aligned} E &= I - I^2/4, \\ \omega &= \partial E / \partial I = \sqrt{(1-E)}. \end{aligned} \quad (\text{A3})$$

If we define

$$z = \omega y / (x - E),$$

then it follows that

$$dz/d\tau = -\omega(1+z^2),$$

which has the following solution

$$\begin{aligned} z &= -\tan(\omega\tau) \\ &= -\tan\theta. \end{aligned} \quad (\text{A4})$$

Finally from Eqs. (A1) and (A4) we obtain the transformation relations (5) of Sec. II.

#### APPENDIX B: NONLINEAR RESONANCE ANALYSIS

In this appendix we shall apply the nonlinear resonance analysis developed by Chirikov and others<sup>9,15</sup> to the study of secondary resonances near the separatrix of a special form of a driven pendulum.

We consider a pendulum under a periodic perturbation described by the following Hamiltonian:

$$\begin{aligned} K(p, \theta, \tau) &= K_0(p, \theta) - \beta \cos(2\theta - \Omega\tau), \\ K_0 &= p^2/4 - 2\omega_0^2 \cos\theta. \end{aligned} \quad (\text{B1})$$

This Hamiltonian has the form of Eq. (10) of Sec. II. The motion on the separatrix of the unperturbed pendulum can be obtained explicitly as

$$\theta_s(\tau) = 4 \arctan(e^{\omega_0\tau}) - \pi, \quad (\text{B2})$$

$$p_s(\tau) = \pm 4\omega_0 \cos(\theta_s/2). \quad (\text{B3})$$

We define the local coordinate  $w$  by

$$w = K_0(p, \theta) - 2\omega_0^2,$$

which measures the distance from the separatrix in unit of energy. By differentiating  $w$  directly and using the equations of motion for the perturbed system, the time evolution of  $w$  is determined by

$$dw/d\tau = -\beta p \sin(2\theta - \Omega\tau). \quad (\text{B4})$$

During the phase oscillation when  $\theta$  goes from 0 to  $2\pi$ , the increments of  $\zeta = \Omega\tau$  and  $w$  for rotation near the separatrix can be, separately, approximated by

$$\delta\zeta = (\Omega/\omega_0) \ln(64\omega_0^2/|w|) \quad (\text{B5})$$

and

$$\delta w = -\beta \int_{-\infty}^{\infty} p_s \sin(2\theta_s - \Omega\tau) \, d\tau. \quad (\text{B6})$$

By inserting (B2) and (B3) into (B6), we obtain the so-called Melnikov-Arnol'd integral, which in the limit  $\Omega/\omega_0 \gg 1$  yields (see the appendix of Ref. 3)

$$\delta w = \mu \sin\zeta_0,$$

where

$$\mu = (16\pi/3)\lambda^4 \beta e^{-\pi\lambda/2},$$

$$\lambda = \Omega/\omega_0,$$

where  $\zeta_0$  denotes the phase  $\Omega\tau_0$  of the driving term at

the instant of  $\theta=0$ . Thus the motion between two consecutive  $\theta=0$  crossings can be described by the following Whisker map:<sup>9,15</sup>

$$\begin{aligned} w_{n+1} &= w_n + \mu \sin \zeta_n, \\ \zeta_{n+1} &= \zeta_n + \lambda \ln(64\omega_0^2 / |w_{n+1}|). \end{aligned} \quad (\text{B7})$$

The map (B7) is equivalent to a Hamiltonian system with the following time-dependent Hamiltonian:

$$\begin{aligned} H(w, \zeta, t) &= w \lambda [\ln(64\omega_0^2 / |w|) + 1] \\ &+ \mu \cos \zeta \sum_{-\infty}^{\infty} \cos(2\pi n t). \end{aligned} \quad (\text{B8})$$

This Hamiltonian displays an infinite sequence of primary resonances. Note that  $\theta$  appears in the new Ham-

iltonian system (B8) as  $2\pi t$ ; thus the resonance condition is given by

$$\zeta = \Omega \tau = n \theta.$$

Hence  $\theta = \Omega \tau / n$ ,  $n = 2, 3, \dots$  gives a sequence of secondary resonances of the original system (B1). By reducing the Hamiltonian (B8) to a pendulum form, we may also estimate the widths of these resonances as given by

$$\Delta w = 4\sqrt{\mu w(n)/\lambda}, \quad (\text{B9})$$

where  $w(n)$  is determined by

$$d\zeta/dt = 2\pi n,$$

which yields

$$w(n) = 64\omega_0^2 e^{-2n\pi/\lambda}. \quad (\text{B10})$$

\*Permanent address: Department of Physics, Lanzhou University, Lanzhou, Gansu, People's Republic of China.

<sup>1</sup>R. B. Walker and R. K. Preston, *J. Chem. Phys.* **67**, 2017 (1971).

<sup>2</sup>K. M. Christoffel and J. M. Bowman, *J. Phys. Chem.* **85**, 2159 (1981).

<sup>3</sup>S. K. Gray, *Chem. Phys.* **75**, 67 (1983).

<sup>4</sup>P. S. Dardi and S. K. Gray, *J. Chem. Phys.* **80**, 4738 (1984).

<sup>5</sup>R. C. Brown and R. E. Wyatt, *Phys. Rev. Lett.* **57**, 1 (1986).

<sup>6</sup>R. B. Shirts and T. F. Davis, *J. Phys. Chem.* **88**, 4665 (1984).

<sup>7</sup>R. M. O. Galvano, L. C. M. Miranda, and J. T. Mendonca, *J. Phys. B* **17**, L577 (1984).

<sup>8</sup>D. Poppe and J. Korsch, *Physica* **24D**, 367 (1987).

<sup>9</sup>B. V. Chirikov, *Phys. Rep.* **52**, 263 (1979).

<sup>10</sup>R. S. Mackay, J. D. Meiss, and I. C. Percival, *Physica* **13D**, 55 (1984).

<sup>11</sup>D. B. Bensimon and L. P. Kadanoff, *Physica* **13D**, 82 (1984).

<sup>12</sup>R. B. Shirts and W. P. Reinhardt, *J. Chem. Phys.* **77**, 5204 (1982).

<sup>13</sup>M. J. Davis and S. K. Gray, *J. Chem. Phys.* **84**, 5389 (1986).

<sup>14</sup>M. J. Davis, *J. Chem. Phys.* **83**, 1016 (1985).

<sup>15</sup>F. Vivaldi, *Rev. Mod. Phys.* **56**, 737 (1984).

<sup>16</sup>J. M. Greene, *J. Math. Phys.* **20**, 1183 (1979).